JOURNAL OF APPLIED ELECTROCHEMISTRY 17 (1987) 489–494

Miniature oxygen pump-gauge. III. Application of a periodic current waveform

W. C. MASKELL, H. KANEKO*, B. C. H. STEELE

Wolfson Unit for Solid State Ionics, Department of Materials Science, Imperial College, Prince Consort Road, London SW7 2BP, UK

Received 24 April 1986

Sinusoidal currents were applied to the pumps of pump-gauge devices constructed from zirconia, enclosing a sealed volume of less than 1 mm^3. Values for the gauge e.m.f. were monitored versus time and compared with theoretical equations derived assuming ideal behaviour. Under a low signal condition, where the amplitude of the gauge e.m.f. was $\leqslant 2.3$ mV (at 800° C), the theory predicted that the e.m.f. should also be sinusoidal but with a $\pi/2$ phase shift relative to the current. Under a high signal condition, on the other hand, where the amplitude of the gauge e.m.f. was > 10 mV, substantial distortion of the e.m.f. variation from a pure sinusoid was anticipated. Observed behaviour was in general closely in accordance with these predictions, although some deviation was apparent at low internal pressures (< 0.01 atm).

1. Introduction

The miniature oxygen pump-gauge in its simplest form consists of two oxygen ion-conducting ceramic discs fixed together to enclose a small, sealed volume. On its flat surfaces each disc has porous metallic electrodes, often platinum, and external connections to those electrodes. One pair of electrodes is used for pumping oxygen electrochemically into and out of the enclosed volume and the other pair is used to determine potentiometrically the ratio of the outer and inner oxygen partial pressures. These devices are versatile, having a number of modes of operation for oxygen sensing. It was shown in Part II [1] that by applying a sinusoidal current to the pump, the internal (reference) oxygen pressure could be determined from the resulting pseudo-sinusoidal variation of the e.m.f. Thus the oxygen content of the sample gas can be monitored continuously, relative to the known reference pressure.

It is the purpose of the present communication to derive the theoretical equations describing the anticipated response of an ideal system to an imposed sinusoidal current, and to compare these with the observed behaviour. Meas [2] reported a related study which was carried out on a pump-gauge with an active internal volume five orders of magnitude larger than the present device, operated at relatively low internal oxygen pressures ($< 10^{-3}$ atm).

2. Theory

A schematic cross-section of the pump-gauge is shown in Fig. 1. Outer and inner oxygen partial pressures are designated as p_1 and p_2, respectively. One half of the cell is used for electrochemical oxygen pumping and the other half (gauge) for potentiometric oxygen sensing. Assuming ideality, i.e. no sorption on internal surfaces, no oxidation–reduction of inner electrodes and negligible changes in stoichiometry of the ceramic, then

$$p_2 V = nRT \quad (1)$$

where V is the internal volume and n the number of moles of O_2 contained. Faraday's law may be expressed as

$$\Delta n = -\Delta Q/4F \quad (2)$$

* *Present address*: Department of Metallurgy, Mining College, Akita University, Akita 010, Japan.

0021–891X/87 $03.00 + .12

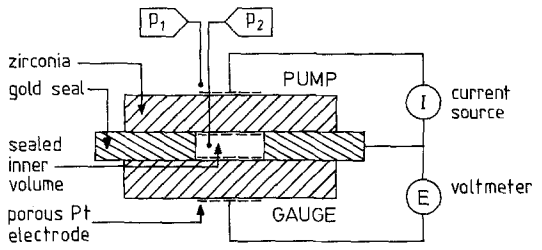

Fig. 1. Pump-gauge device.

where Q is the charge passed with the convention that a positive current, I, pumps oxygen out of the device: R, T and F have their usual significance. It follows that

$$(\mathrm{d}p_2/\mathrm{d}t) = -(RT/4FV)I \quad (3)$$

and

$$p_2 = -(RT/4FV)\int I\mathrm{d}t \quad (4)$$

Equation 4 predicts the internal oxygen pressure as a function of time, t, for any given current waveform. For the specific case of a sinusoidal waveform

$$I = A \sin \omega t \quad (5)$$

where A is the amplitude and ω the angular frequency ($\omega = 2\pi f$ where f is the frequency). From Equations 4 and 5

$$p_2 = (RTA/4FV\omega) \cos \omega t + p_0 \quad (6)$$

where p_0 is a constant equal to the mean oxygen pressure inside the device, i.e. the average value of p_2. The cell e.m.f., E, is given by

$$E = (RT/4F) \ln p_1/p_2 \quad (7)$$

assuming rapid response of electrodes to changes in p_1 and p_2. Substituting for p_2 from Equation 6

$$E = (RT/4F) \ln (p_1/p_0) - (RT/4F) \ln \left(1 + \frac{RTA}{4FV\omega p_0} \cos \omega t\right) \quad (8)$$

Writing

$$E_0 = (RT/4F) \ln (p_1/p_0) \quad (9)$$

Equation 8 becomes

$$E = E_0 - (RT/4F) \ln \left(1 + \frac{RTA}{4FV\omega p_0} \cos \omega t\right) \quad (10)$$

This is the general theoretical equation for the variation of the e.m.f. resulting from the application of a sinusoidal current. It may be simplified for $RTA/4FV\omega p_0 \leqslant 0.1$ by the approximation

$$E = E_0 - (RT/4F)^2 (A \cos \omega t/V\omega p_0) \quad (11)$$

Clearly, Equation 11 predicts a phase shift of $\pi/2$ between the e.m.f. and the current (compare Equation 5). $RTA/4FV\omega p_0 \leqslant 0.1$ corresponds to an amplitude of the e.m.f. of $\leqslant 2.3$ mV at 800° C.

The above theory ignores leakage effects [3], which is acceptable under appropriate conditions (i.e. relatively high currents and frequencies and, where necessary, a bias current applied equal and opposite to the mean leakage current). The work to be described involves verification of Equations 10 and 11.

3. Experimental details

The device used in the majority of the work was constructed of partially stabilized zirconia (PSZ). A few measurements were made using a pump-gauge fabricated from single crystal zirconia (SCZ). The fabrication of these sensors and other experimental details were as previously described [1, 3]. Currents were imposed using a potentiostat in the galvanodynamic mode taking the signal from a function generator. This ensured that the currents were truly sinusoidal as impedance variations (non-linear characteristic) of the pump did not influence the magnitude of the current. The pump-gauge devices were operated at 800 ± 2° C. Gas mixtures of O_2 and N_2 were calibrated using a sampling potentiometric oxygen gauge with air reference operated at 700° C.

4. Results and discussion

The pump-gauge was first operated at constant frequency (0.1 Hz) in air ($p_0 \simeq p_1 = 0.21$ atm)

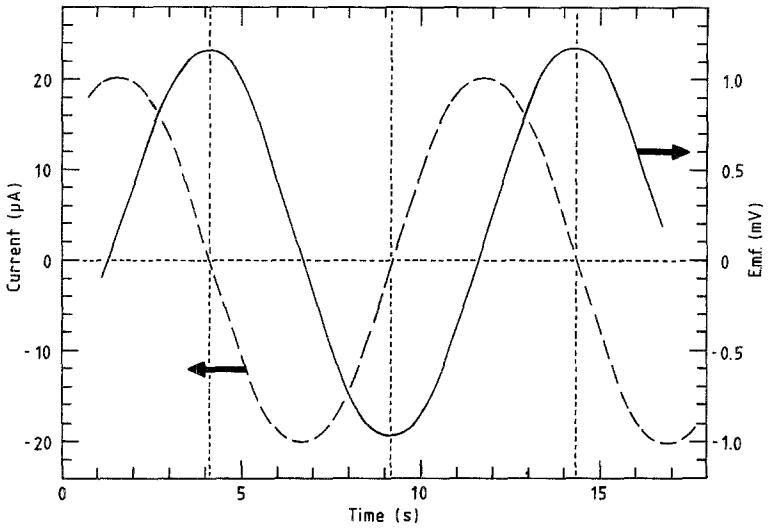

Fig. 2. Gauge e.m.f. versus time with sinusoidal pump current for PSZ device at 800° C in air.

and the amplitude of the gauge e.m.f., B, measured for a range of current amplitudes. Fig. 2 is a typical recording showing current and e.m.f. versus time. A phase shift of $\pi/2$ (compare Equations 5 and 11) was revealed by the broken line drawn through points of zero current. Equation 11 predicts

$$B = (RT/4F)^2 A/V\omega p_0 \qquad (12)$$

A plot of the amplitude of the e.m.f. versus Ap_1/p_0 (with p_1 and ω constant) is shown in Fig. 3; p_0 was determined from the average e.m.f. using Equation 9. For all the points shown p_1/p_0 was close to unity (± 0.01). The straight line behaviour was compatible with Equation 12.

In the next series of measurements the device was again operated in air ($p_0 \simeq p_1 = 0.21$ atm), but sinusoidal frequency was varied while the current amplitude was maintained constant at 10 μA. A linear relationship between e.m.f. amplitude and $p_1/\omega p_0$ (with p_1 and A constant) was found (Fig. 4). Again the deviation of p_1/p_0 from unity was small (± 0.05). In both Figs 3 and 4 proportionality between the amplitude of the e.m.f. and either current amplitude or recipro-

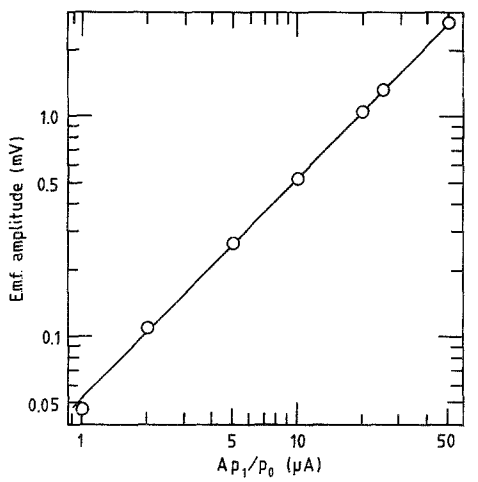

Fig. 3. Plot of B versus Ap_1/p_0; details as Fig. 2. Line shown has unit slope.

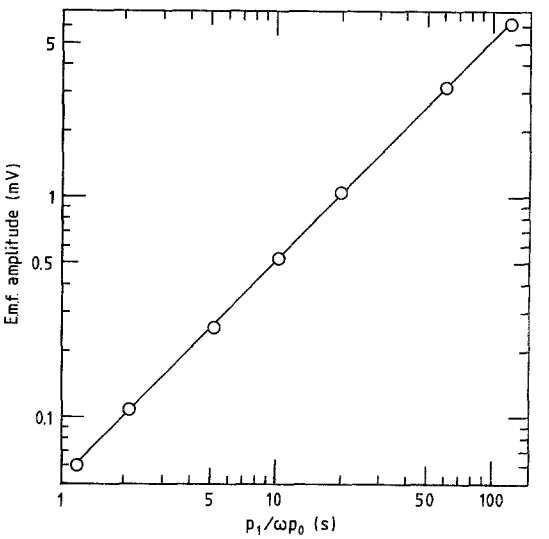

Fig. 4. Plot of B versus $p_1/\omega p_0$; details as Fig. 2. Line shown has unit slope.

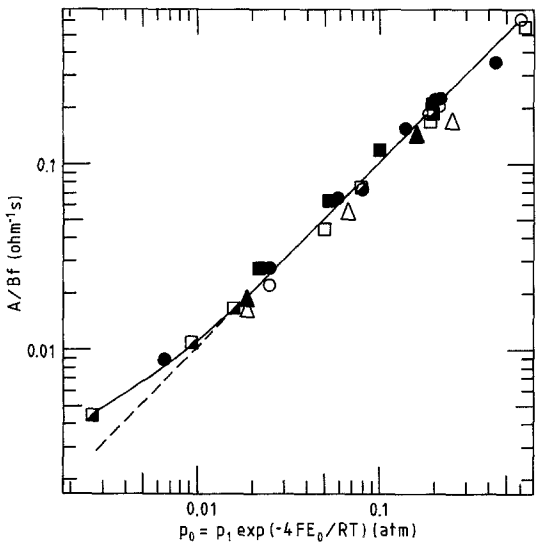

Fig. 5. Plot of A/Bf versus p_0 (calculated from E_0) for PSZ device at 800° C with $B \leqslant 2.3$ mV. Values of p_1 (atm)/f(Hz): ○, 0.21/0.093; ●, 0.21/0.64; □, 0.022/0.041; ◪, 0.022/0.25; ■, 0.022/0.71; △, 0.022/0.16; ▲, 0.022/0.37. Line shown has unit slope.

cal frequency was demonstrated over two orders of magnitude in agreement with the theory (Equation 12).

As a further test of Equation 11 the parameters p_1, p_0 ($p_0 \neq p_1$), A and ω were varied while the amplitude of the e.m.f. was maintained in the range 0.08–2.3 mV. The ratio of p_1/p_0 was varied between 10^{-2} and 10^2 by applying a d.c. bias to the a.c. voltage (facility available on the function generator) to balance the appropriate leakage current [3]. This equilibrium was achieved when the mean e.m.f. remained constant [1]. In these measurements, shown in Fig. 5, p_1 was varied in the range 0.0022–0.21 atm. In this log–log plot the data were again well described by a straight line of unit slope indicating linearity between A/Bf and p_0 in conformance with Equations 11 and 12. Some deviation from the theoretical line was apparent for $p_0 < 0.01$ atm in Fig. 5. This suggests that at low internal pressures the assumption of ideality was no longer valid. A possible explanation is that the response time of the internal gauge electrode increased with decreasing oxygen pressure [4] to the point where the gauge could no longer follow the oxygen pressure changes at the applied frequency sufficiently rapidly.

The internal volume of the device was calculated from the intercepts of the lines in Figs 3–5 and these values are compared in Table 1 with the volume determined by application of a constant imposed pumping current as described in Part I [3]. A probable error has been included with the value obtained from Fig. 5 because the data showed more scatter than those in the other figures. This scatter was thought to have resulted from the sometimes large ratio between p_0 and p_1 which entailed the application of bias currents.

Table 1. Comparison of values for the internal cell volume determined by various methods

Determination	*Internal cell volume (mm^3)*	
	PSZ device	*SCZ device*
Constant current technique (Fig. 8 of [3]) with $p_1 = 0.21$ atm.	0.77	0.65
Current amplitude varied (Fig. 3) $p_0 \simeq p_1 = 0.21, f = 0.1$ Hz	0.78	
Frequency varied (Fig. 4) $p_0 \simeq p_1 = 0.21, A = 10\,\mu$A	0.76	
All parameters varied (Fig. 5) $p_0 \neq p_1$, $B \leqslant 2.3$ mV	0.87 ± 0.14	
E.m.f. amplitude $\gg 10$ mV (Fig. 7a) $f = 0.1$ Hz, $A = 400\,\mu$A.		0.66
E.m.f. amplitude $\gg 10$ mV (Fig. 7b) $f = 0.1$ Hz, $A = 200\,\mu$A.		0.63

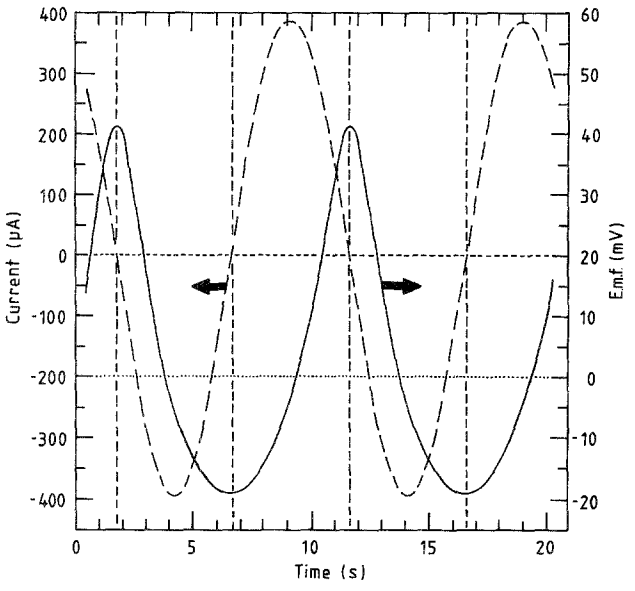

Fig. 6. Gauge e.m.f. (amplitude > 10 mV) versus time with sinusoidal pump current ($A = 400\,\mu A$) for SCZ device at 800° C in air at 0.1 Hz.

Consequently, it was more difficult to achieve a stable equilibrium situation than when $p_0 \simeq p_1$. Table 1 shows good agreement between the volumes determined from the four sets of data, providing additional confirmation of the validity of Equation 11.

Finally, conformance of the behaviour of the pump-gauge to Equation 10 for large amplitude of the e.m.f. (> 10 mV) was investigated. The distortion of the e.m.f. from a sine wave is apparent in Fig. 6. The value of E_0 (Equations 9 and 10) was first determined as the e.m.f., E, when cos ωt was zero (Equation 8): clearly this corresponded to maximum values of $|I|$ (Equation 5) because the phase shift between I and E was $\pi/2$ within experimental error (Fig. 6). Equations 8 and 9 may be rewritten as follows:

$$\exp\,[(4F/RT)(E_0 - E)] = 1 + (RTA/4FV\omega p_0)\cos\omega t \qquad (13)$$

Plots of exp $[(4F/RT)(E_0 - E)]$ versus cos ωt are shown in Fig. 7. The data displayed straight

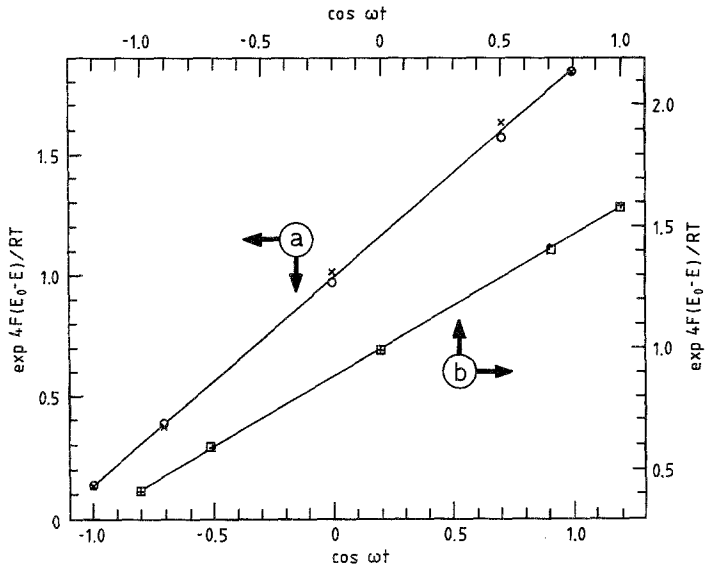

Fig. 7. Plots of exp $[(4F/RT)(E_0 - E)]$ versus cos ωt (Equation 13) for SCZ device at 800° C in air at 0.1 Hz. (a) $A = 400\,\mu A$, $p_0 = 0.259$ atm; (b) $A = 200\,\mu A$, $p_0 = 0.197$ atm. □, ○, cos ωt decreasing; †, ×, cos ωt increasing.

line behaviour as expected from Equation 13, showing that Equation 8 was being closely obeyed. The small deviations in Fig. 7 for the data corresponding to a current amplitude of 400 μA were attributed to significant leakage of oxygen at high values of $|E|$ [3]. Internal cell volumes determined from the slopes of the lines in Fig. 7 are presented in Table 1: these were in excellent agreement with the value determined from the technique involving the imposition of constant currents of 5–80 μA [3].

5. Conclusions

The miniature oxygen pump-gauge demonstrated behaviour close to ideal over a substantial range of conditions of applied input current, frequency and internal and external pressures. There were indications of deviations for internal oxygen pressures below 0.01 atm, possibly due to the onset of increasing electrode response times at low internal pressures. Further work should be aimed at investigating behaviour at low internal pressures (< 0.01 atm), at higher frequencies (> 1 Hz) and with devices constructed from alternative ceramics, e.g. Bi_2O_3.

References

[1] W. C. Maskell, H. Kaneko and B. C. H. Steele, Part II, Proc. 2nd Int. Symp. Chemical Sensors, Bordeaux, 7–10 July 1986, Bordeaux Chemical Sensors, University of Bordeaux, pp. 302–5.
[2] Y. Meas, PhD Thesis, University of Grenoble (1978).
[3] H. Kaneko, W. C. Maskell and B. C. H. Steele, Part I, *Solid State Ionics*, in press.
[4] J. Fouletier, H. Seinera and M. Kleitz, *J. Appl. Electrochem.* **4** (1974) 305.